

TERRA/AQUA データによる汚濁水塊のスペクトル特性評価（その 3）

岩下圭之（土木工学科）、大木宜章（土木工学科）、J.C.Dozier（UCSB）

1.Introduction

本プロジェクトのこれまでの成果として、ハーパースペクトル計測による各水質項目に応じた「有効波長帯」の選定、ならびにそれを応用した LandsatTM または Terra/ASTER などの高解像度衛星に対する「複合ラジオメトリック補正法」: Filament-Shaped Method の構築を行って成果を得てきた。これらの知見をベースに、平成 19 年度の達成目標であるハーパースペクトル計測衛星 Terra/Aqua データへの「複合ラジオメトリック補正法」の適用について再度ハーパースペクトル現地計測を基本に行ってきた。

本年度は、研究の方向を次のとおり 2 通りに分けて行い、完成結果を報告する。

1) Algorithm for Combined Radiometric Correction

11 月から 3 月まで米国カリフォルニア大学サンタバーバラ校との共同で数回行った、「汚濁水塊を対象としたハーパースペクトル」の現地(Santa Monica Bay & Long Beach port)計測において SS 混在の植物プランクトンがスペクトルノイズの主要因となっている事が判明し、低解像度 Terra/AQUA 用の「複合ラジオメトリック補正法」再構築の大きな指針となった。(* 英文)

2) Time-Series Satellite Analysis

多時期の高解像度衛星データを利用して、他の水質項目、特に水底堆積土に代表される SS や化学的酸素要求量 (Chemical Oxygen Demand: 以降 COD) のような無機懸濁物の推定モデルを構築し、これを利用して手賀沼の水質変動の約 3 5 年スパンの時系列的解析を行った。

2. Algorithm Theoretical Analysis

2.1 R_{rs} Model

The R_{rs} model is given by the following general equation, which is adapted from previous

methods:

$$R_{rs}(\lambda) = f t^2 / Q(\lambda) \times b_b(\lambda) / [a(\lambda) + b_b(\lambda)] \dots (1)$$

where f is an empirical factor averaging about 0.32-0.33 [Gordon et al., 1975; Morel and Prieur, 1977; Jerome et al., 1988; Kirk, 1991], t is the transmittance of the air-sea interface, $Q(\lambda)$ is the upwelling irradiance-to-radiance ratio $E_u(\lambda)/L_u(\lambda)$, and n is the real part of the index of refraction of seawater. By making three approximations, (1) can be greatly simplified.

1) In general, f is a function of the solar zenith angle, θ_0 [Kirk, 1984; Jerome et al., 1988; Morel and Gentili, 1991]. However, Morel and Gentili [1993] have shown that the ratio f/Q is relatively independent of θ_0 for sun and satellite viewing angles expected for the MODIS orbit. They estimate that $f/Q = 0.0936, 0.0944, 0.0929,$ and $0.0881,$ (standard deviation ≈ 0.005), for $\lambda = 440, 500, 565,$ and 665 nm, respectively. Also, Gordon et al., [1988] estimates that $f/Q = 0.0949$, at least for $\theta_0 > 20^\circ$. Thus, we assume that f/Q is independent of λ and θ_0 for all Terra/ASTER wavebands of interest, except perhaps for the band centered at 667 nm, which we do not use.

2) t^2/n^2 is approximately equal to 0.54, and although it can change with sea-state (Austin, 1974), it is relatively independent of wavelength.

3) Many studies have confirmed that $b_b(\lambda)$ is usually much smaller than $a(\lambda)$ and can thus be safely removed from the denominator of following (2) [Morel and Prieur, 1977; references cited in Gordon and Morel, 1983], except for highly turbid waters.

These three approximations lead to a simplified version of (1),

$$R_{rs}(\lambda) \approx \text{constant } b_b(\lambda) / a(\lambda) \dots (2)$$

where the "constant" is unchanging with respect to λ and θ_0 . The value of the constant is not relevant to the algorithm since the algorithm uses spectral ratios of $R_{rs}(\lambda)$ and the constant term factors out.

In the following sections, both $b_b(\lambda)$ and $a(\lambda)$ will be divided into several separate terms. Each term will be described empirically. The equations are written in a general fashion-i.e., the empirically derived parameters that describe each term are written as variables C and the actual values of the parameters that are used in the algorithm are shown in Tables 1a and 1b.

Table 1a Wavelength-Dependent Parameters for the semi-analytical Chlorophyll Algorithm for lake

λ	412(nm)	443(nm)	488(nm)	551(nm)
a0	2.22	3.59	2.27	0.42
a1	0.74	0.8	0.59	-0.22
a2	-0.5	-0.5	-0.49	-0.5
a3	0.0013	0.0111	0.0112	0.0111
bbw(m-1)	0.003339	0.002459	0.001561	0.000929
aw(m-1)	0.00478	0.00744	0.01633	0.0591

Table 1b Wavelength-Independent Parameters for the semi-analytical Chlorophyll Algorithm for lake

wavelength independent parameter					
X_0	-0.00182	S	0.0225	C_0	0.2818
X_1	2.058	p_0	51.9	C_1	-2.783
Y_0	-1.13	p_1	1	C_2	1.863
Y_1	2.57			C_3	-2.387

2.2 Back Scattering Term

The total backscattering coefficient, $b_b(\lambda)$ can be expanded as

$$b_b(\lambda) = b_{bw}(\lambda) + b_{bp}(\lambda) \dots (3)$$

where the subscripts "w" and "p" refer to water and particles, respectively. $b_{bw}(\lambda)$ is constant and well known [Smith and Baker, 1981]. $b_{bp}(\lambda)$ is modeled as

$$b_{bp}(\lambda) = X[551/\lambda]^Y \dots (4)$$

The magnitude of particle backscattering is indicated by X, which is equal to $b_{bp}(551\text{nm})$, while Y describes the spectral shape of the particle backscattering.

Lee et al., [1994] empirically determined X and Y values by model inversion using a formula similar to (4). The X and Y values were compared to the $R_{rs}(\lambda)$ values measured at each station with the purpose of finding empirical relationships for both X and Y as a function of $R_{rs}(\lambda)$ at one or more of the Terra/AQUA wavelengths. Once this was done, X and Y could be estimated from satellite data using following formula.

Expression for X;

$$X = X_0 + X_1 * R_{rs}(551) \dots (5)$$

where X_0 and X_1 are empirically derived constants. Linear regression performed on the derived values of X vs. $R_{rs}(551\text{nm})$ taken from six observation of the Lake Inbanuma & experimental pond at Nihon University resulted in X_0 and X_1 values of 0.00182 and 2.058 ($n = 53$, $r^2 = 0.96$). Figure 1

shows the regression graphically. If X is determined to be negative from 式 5 it is set to zero.

Expression for Y;

Y was found to covary in a rather general way with the ratio $R_{rs}(443\text{nm})/R_{rs}(488\text{nm})$. Variations in numerator and denominator values of this ratio are largely determined by absorption due to phytoplankton and CDOM. Absorption due to water is about the same and low at both wavelengths. Thus, to the extent that phytoplankton and CDOM absorption covary, the spectral ratio of the absorption coefficients, $a(443\text{nm})/a(488\text{nm})$, will be only weakly dependent on pigment concentration, and the spectral ratio of backscattering coefficients should have a significant effect on the spectral ratio of R_{rs} . Y is thus

represented as

$$Y = Y_0 + Y_1 * R_{rs}(443)/R_{rs}(488) \dots (6)$$

a linear function of $R_{rs}(443\text{nm})/R_{rs}(488\text{nm})$ where Y_0 and Y_1 are empirically derived constants.

These empirical relationships are shown in Fig.1(a) & (b).

2.3 Absorption Term

The total absorption coefficient can be expanded as

$$a(\lambda) = a_w(\lambda) + a_\phi(\lambda) + a_d(\lambda) + a_g(\lambda) \dots (7)$$

where the subscripts "w", " ϕ ", "d", and "g" refer to water, phytoplankton, detritus, and CDOM ("g" stands for gelbstoff). Here $a_w(\lambda)$ is taken from Pope and Fry, [1997]. Expressions for $a_\phi(\lambda)$, $a_d(\lambda)$, and $a_g(\lambda)$ are omitted for limited space.

2.4 Weighted Chl-a Pigment Algorithm

Another consideration is that there should be a smooth transition in [chl a] values when the algorithm switches from the semi-analytical to the empirical method. This is achieved by using a weighted average of the [chl a] values returned by the two algorithms when near the transition border. When the semi-analytical algorithm returns an $a_\phi(675\text{nm})$ value between 0.015 and 0.03 m^{-1} , [chl a] is calculated as

$$[chl a] = w [chl a]_{sa} + (1-w) [chl a]_{emp} \dots (8)$$

where $[chl a]_{sa}$ is the semi-analytically-derived value and $[chl a]_{emp}$ is the empirically derived value, and the weighting factor is;

$$w = [0.03 - a_\phi(675)] / 0.015.$$

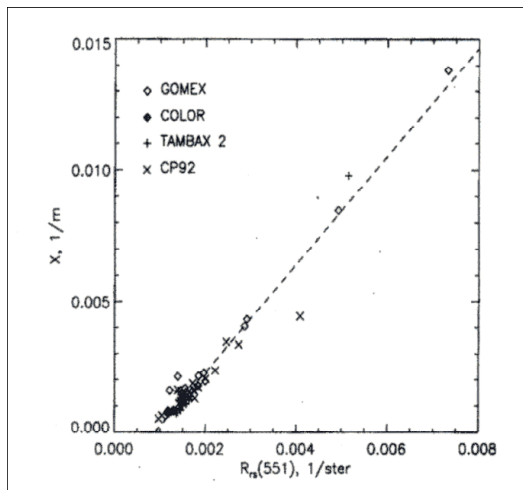


Fig. 1a X versus Rrs(551nm; visible green), where X is the magnitude of particle backscattering and Rrs is the Terra/Aster L1b data reflectance at 551 nm. The line is the linear regression equation;
 $X = -0.00182 + 2.058 Rrs(551nm)$ ($n=53$, $r^2=0.96$)

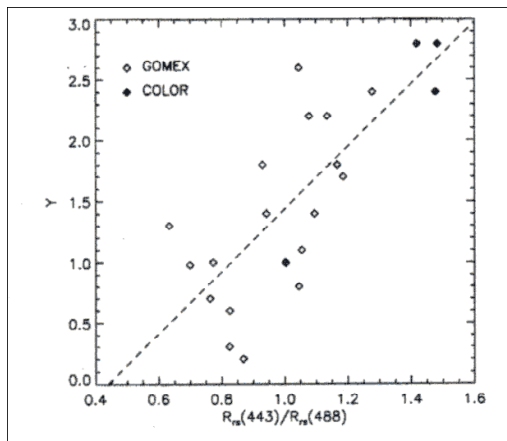


Fig. 1b Spectral shape of particle backscattering Y versus Rrs(443nm)/Rrs(488nm). The line is the linear regression;
 $Y = -1.13 + 2.57 Rrs(443nm)/Rrs(488nm)$ ($n=22$, $r^2=0.59$)

2.5 Algorithm Evaluation

Several data sets within the low resolution coverage wide area evaluation set were numerically diagnosed as coming from waters where the pigments were much more packaged than those from the warm, tropical and subtropical data sets evaluated earlier. The new packaged parameters are used to define a slightly different, packaged algorithm for upwelling and winter-spring temperate regions.

There are 326 points in an ensemble of multiyear, multiseason data sets from the California Current which we label as packaged. These consist of historical CalCOFI ($n=303$) and recent Cal9704 ($n=23$) data which we recently

collected with G. Mitchell. The CalCOFI Rrs data were subsurface measurements, while the Cal9704 data were above-surface collections. Three hundred and three points (93%) from this packaged data set passed the semi-analytical portion of the new algorithm, yielding RMS1 and RMS2 errors for [chl a] retrieval of 0.111 and 0.268, respectively. The type II RMA slope was 0.999, the bias was -0.006, and the r^2 value was 0.917. The scatter plot overlays the one-to-one line, and the quantile plot is linear and overlies the one-to-one line but has a slight discontinuity near a chlorophyll value of 3. This indicates that some parameter modifications for the packaged algorithm are needed in this transition region.

Using the blended algorithm on 326 data points, the r^2 increased to 0.951 while the other statistics remained about the same. The RMS2 error of about 28% for the packaged algorithm also is better than our accuracy goal of 35% or less.

3. A Time-Series Satellite Analysis

3.1 Water-leaving Radiance Measurements

Water-leaving radiance was measured Field-Spec Hyper-spectral radiometer with bandwidths of 1nm that synchronize with four bands in the visible, and one band in the near infrared(NIR) at 750 nm of the LANDSAT ETM and ASTER data. The four bands possessed high radiometric sensitivity (well over an order of magnitude higher than other sensors designed for earth resources, e.g., normal spectro-meter for the TM & MSS on the Landsat series) and were specifically designed for water color. The field experience demonstrated the feasibility of the measurement of phytoplankton pigments, and possibly even productivity on a local scale. This feasibility rests squarely on several field observations:

(1) there exists a more relationship between the water color and the phytoplankton pigment (Chl-a) concentration for most open waters.

(2) it is possible to develop algorithms to remove the interfering effects of the atmosphere from the imagery.

In next step we will accomplish the multi algorithm for removing the atmospheric effects from Terra/Aqua

and MODIS imagery over the ocean to derive the

normalized water-leaving radiance in the visible. The process of deriving the normalized water-leaving radiance from imagery of the water body is usually termed atmospheric correction.

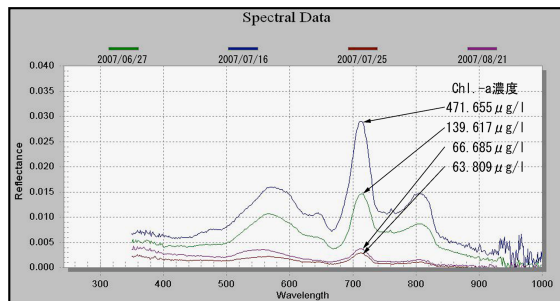


Fig. 2 Hyper-spectral of Chl-a content water-body (fields work by FieldSpcePro)

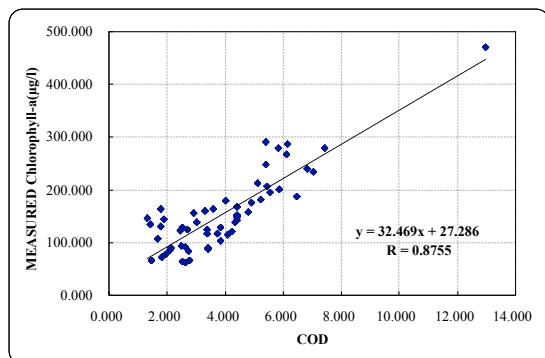


Fig.3 Comparison between measured Chl.-aand COD

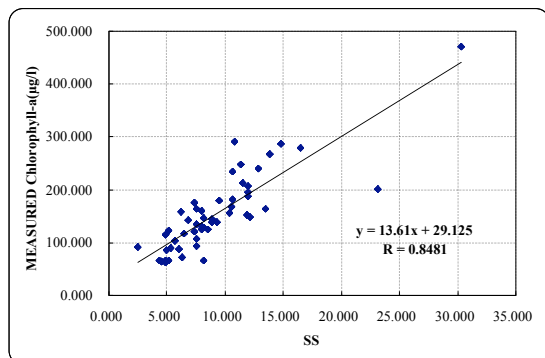


Fig.4 Comparison between measured Chl.-a and SS

References

- 1) Aiken, J., G.F. Moore, C.C. Trees, S.B. Hooker, and D.K. Clark, The SeaWiFS CZCS-type pigment algorithm, in SeaWiFS Technical Report Series, vol. 29, edited by S.B. Hooker and E.R. Firestone, Goddard Space Flight Center, Greenbelt, MD, 1995.
- 2) Arrigo, K.R., D.H. Robinson, D.L. Worthen, B. 21,683-21,695, 1998.
- 3) Behrenfeld, M.J. and P.G. Falkowski, Photosynthetic rates derived from satellite-based chlorophyll concentration, *Limnol. Oceanogr.*, 42, 1-20, 1997.

3.2 Time-Series Satellite Analysis for TSI -featuring “Filament-Shaped Method”-

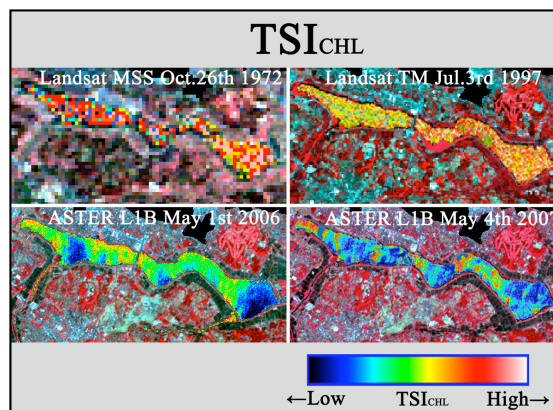


Fig. 5(a) Time-series Mapping for TSI Chl-a

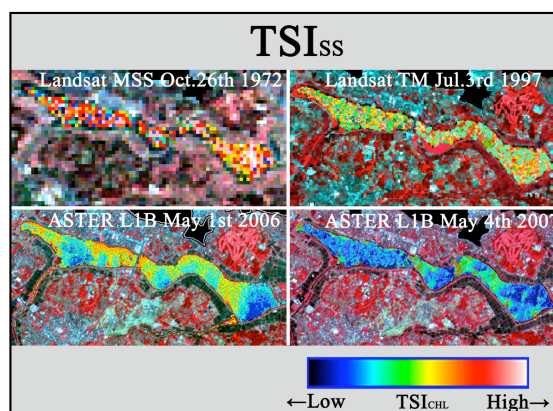


Fig. 5(b) Time-series Mapping for TSI SS

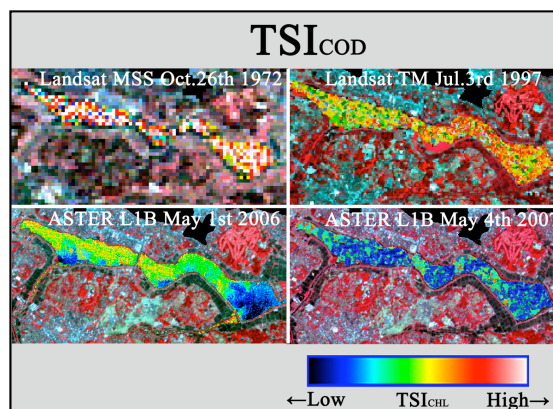


Fig. 5(c) Time-series Mapping for TSI COD

- 4) Brody, E., B.G. Mitchell, O. Holm-Hansen, and M. Vernet, Species-dependent variations of the absorption coefficient in the Gerlache Strait, *Antarctic Journal*, 27, 160-162, 1992.
- 5) Carder, K.L., F.R. Chen, J.P. Cannizzaro, J.W. Campbell, and B.G. Mitchell, Performance of MODIS semi-analytic ocean color algorithm for chlorophyll-a, *Advances in Space Research*, in press, 2003.

